Development of heat-sensitive microbubbles for cancer ablation margin assessment

Jiwei Huang

Department of Biomedical Engineering, The Ohio State University, Columbus, OH 43210

Abstract:

Thermal ablation processes hold the promise of less invasive cancer management. But broader acceptance of cancer ablation processes is hindered by controversial issues and concerns due to the lack of effective assessment of the ablation margin during surgery. We developed heat-sensitive microbubbles for ablation margin assessment during a cancer ablation surgery. The heat-sensitive microbubbles, which comprise a core of liquid perfluorocarbons (PFC) within a biodegradable poly lactic-co-glycolic acid (PLGA) shell, were fabricated using an emulsion evaporation method. Optical microscopic imaging showed that, at the boiling point of PFC (55ºC), the microbubbles expanded from 1 μm to 20 μm due to PFC evaporation. Additionally, the microbubbles were embedded in a tissue simulating phantom made of agar-agar gel for ultrasound imaging. At room temperature, the microbubbles were not detected by the ultrasound. After being evenly heated to 55 ºC for 10 minutes, the microbubbles were clearly visualized by the ultrasound. These results demonstrate that the heat sensitive microbubbles can be potentially utilized as an ultrasound contrast agent for thermal ablation margin assessment. Successful implementation of these heat-sensitive microbubbles may enhance the accuracy for cancer ablation and revolutionize the clinical practice of cancer management.

Keywords:

microbubble, thermal ablation, intraoperative imaging, heat-sensitive, ablation margin, ultrasound

1. Introduction

Thermal ablation is a minimally-invasive technique for cancer treatment that has received increasing interests in recent years. As an alternative to traditional surgical intervention for cancer treatment, thermal ablation uses heat to destroy cancerous tissue and the surrounding margin. Several thermal ablation techniques have been implemented clinically, including radiofrequency (RF) ablation[1], laser ablation[2], High Intensity Focused Ultrasound (HIFU) ablation [3], and microwave ablation[4]. Thermal ablation holds the promise of less invasive cancer management with outpatient treatments, minimal trauma, minimal side effects and short recovery time[5, 6]. However, broader acceptance of cancer ablation processes is hindered by controversial issues and concerns related with clinical safety, efficacy, and long-term local recurrence[7, 8]. These concerns are due to the lack of effective assessment of the ablation margin during the thermal ablation therapy[5, 6, 8].

Thermal ablation destroys the tumor tissue by localized deposition of thermal energy that causes protein denaturation and coagulation necrosis. At the typical ablation temperature ranging from 50^{o} C to 100^{o} C, irreversible tissue damage occurs after 2 minutes of heating [5]. The ablation margin (i.e., the region of effective tissue destruction) can be defined by the 50–54^{o} C contour and a 'lethal thermal dose', which can be determined by both tissue temperature and thermal exposure time[5]. The lethal thermal dose varies with tissue types,

with a typical value of 240–540 min at 43° C (t_{43}>240–540 min). For complete destruction of tumor, the tumor plus a 1 cm margin of surrounding normal tissue should be ablated[6]. Incomplete ablation may lead to local recurrence which is the re-growing of residual cancerous cells into tumor. In this regard, it is important to monitor the thermal dose and the ablation margin during a thermal ablation therapy.

Existing methods for the assessment of ablation-induced tissue damage include MR thermometry, MR elastography, and visible light spectroscopy [9-11]. These methods do not provide reliable assessment of ablation margins. For example, MR thermometry records the transient tissue temperature map [3, 11-15] and the necrotic margin is estimated based on the Arrhenius model that counts both amplitude and duration of heating [12]. However, disagreement was observed between MR thermal dose maps and actual lesion sizes [16], possibly due to the accumulative errors in numerical models and temperature measurements. Besides, MR thermometry has the following limitations: (1) it is susceptible to motion artifact and tissue swelling[14, 15, 17]; (2) it has low sensitivity in fat tissue[18]; (3) it requires custom design of the thermal therapy system; (4) it's size is large and cost is high.

To overcome the above limitations, we are currently developing heat-sensitive microbubbles for real-time, motion insensitive, intraoperative imaging and assessment of cancer ablation margin. Heat-sensitive microbubbles conjugated with tumor specific biomarkers will target the tumor receptors and deposit at the tumor site after intravenous administration. During thermal ablation, microbubbles will expand at the lethal thermal dose to significantly enhance ultrasound contrast, enabling direct visualization of ablation margin using clinical ultrasound.

This paper summarizes our current work on heat-sensitive microbubbles. The heat-induced

microbubble expansion has been visualized by optical microscopic imaging. The feasibility of using heat-sensitive microbubbles for cancer ablation margin assessment has been demonstrated using tissue-simulating phantom and ultrasound imaging.

2. Materials and methods

2.1 Materials

Poly lactide-co-glycolide (PLGA) was obtained from Boehringer Ingelheim (Ingelheim, Germany). Sodium cholate was purchased from Sigma-Aldrich Chemical Co. (St. Louis, MO). Methylene chloride (CH_2Cl_2) was provided from Fishers Scientific (Newton, NJ). 1,1,1,2,3,4,4,5,5,5-Decafluoropentane was purchased from Fluka (St. Louis, MO). Since 1,1,1,2,3,4,4,5,5,5-Decafluoropentane is one type of perfluorocarbons (PFC) compounds, it will be denoted as PFC in the following text for convenience. Ultrapure deionized water was generated by NANOpure Infinity water purification system (Barnstead International, Dubuque, IA).

2.2 Fabrication of PFC encapsulated PLGA microbubbles

PFC encapsulated PLGA microbubbles were fabricated by a modified emulsion evaporation method [19]. 25mg PLGA was dissolved in 2mL methylene chloride (CH_2Cl_2). Then 1mL PFC was added into the PLGA solution. The solution was then mixed into to 20mL 1.5 w/v% sodium cholate which acted as a surfactant. The final mixture was emulsified using a model 17105 Omni Mixer homogenizer (Omini International, Waterbury, CT) at 20,000 rpm for 2 minutes. After that, the emulsion was stirred by a magnetic bar for 3 hours for evaporation of

CH_2Cl_2. Finally, the mixture was centrifuged by Centrifuge 5810R (Eppendorf, Hamburg, Germany) at 300 rpm for 5 minutes. After centrifugation, the supernatant was discarded, and the microbubble precipitate was saved and re-dispersed by the deionized water. The process of centrifugation and re-dispersing was repeated for three times. The microbubbles were then harvested and stored in deionized water for further use.

2.3 Optical imaging and size distribution of microbubbles

A Nikon TMS-F inverted optical microscope (Melville, NY) was used to visualize and monitor the heat-induced expansion of the PFC encapsulated PLGA microbubbles. A drop of microbubbles dispersed in water was put on the bottom of a cell culture dish and covered by a cover slip. It was made sure that no air bubble was under the cover slip. The surrounding of the cover slip was gently sealed by tape to prevent any leaking of the microbubble solution. The dish was then fixed to the right position under the microscope and images of microbubbles before expansion were recorded. After that, 55^{o} C water was filled into the dish and circulated between the dish and an ISOTEMP 215 water bath (Fisher Scientific) using a water pump (Cole-Parmer Instrument Inc, Chicago, IL). The microscopic image of heated microbubbles was recorded. Size distribution of the microbubbles before and after heating was calculated using image processing and analysis software ImageTool (UTHSCSA, version 3.0).

2.3 Tissue-simulating phantom and ultrasound imaging

Heat-induced expansion of PFC encapsulated PLGA microbubbles was validated using tissue

simulating phantom and ultrasound. The phantom was made by agar-agar gel (Barry Farm, Wapakoneta, OH) with a gelling temperature of 32ºC and melting temperature of 65ºC. 0.1g agar-agar gel powder was fully dissolved in 10mL 70ºC water in a 10mL beaker. As the temperature of agar-agar gel dropped to 37ºC, 150μL microbubble suspension (0.5mg/mL) was added to the gel and fully mixed by a glass stir bar. The mixture was then put inside a refrigerator for complete gelling. After that, the phantom was heated at 55ºC for 10 minutes inside a water bath. Ultrasound images were recorded before and after heating using a Terason 2000 ultrasound probe (Teratech Corp., Burlington, MA). As comparison, a control phantom was made following the identical recipe except that microbubble suspension was not added. The control phantom was heated at the same condition as that of the sample phantom. Ultrasound images of the control phantom were recorded before and after heating.

3. Results

Optical microscopic images of PFC encapsulated PLGA microbubbles before and after heating are shown in Fig.1. Corresponding size distributions of the microbubbles are shown in Fig.2. The mean radius of the microbubbles before heating is 1.26±0.51μm. After being heated at 55ºC for 10 minutes, the microbubbles exploded and expanded to 20.76±10.44 μm due to the evaporation of PFC. It was observed that the explosion of each bubble was instantaneous, and the adjacent microbubbles expanded and merged to form larger microbubbles. The coalescence of microbubbles contributed to the bubble size of greater than 20 μm in the size distribution plot (Figure 2). At the current stage of technology development, the exact thermal dose for microbubbles expansion was not measured due to the complex heat

transfer. However, a mathematical model will be developed and validated for the estimation of the required thermal dose for microbubble expansion, as being further discussed in the later section.

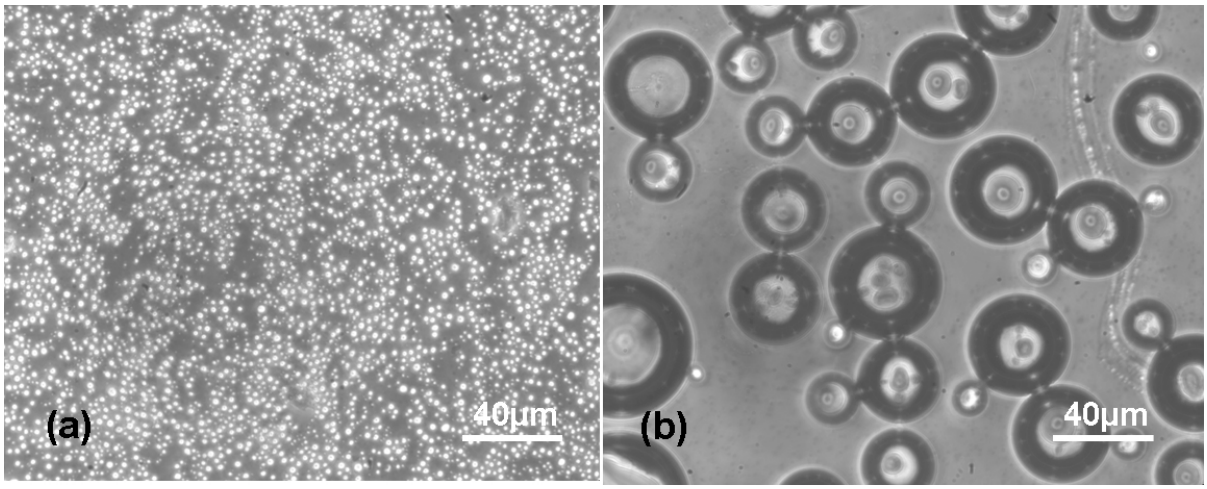

Figure 1. Microscopic image of PFC encapsulated PLGA microbubbles
(a) Before being heated to 55ºC; (b) After being heated to 55ºC

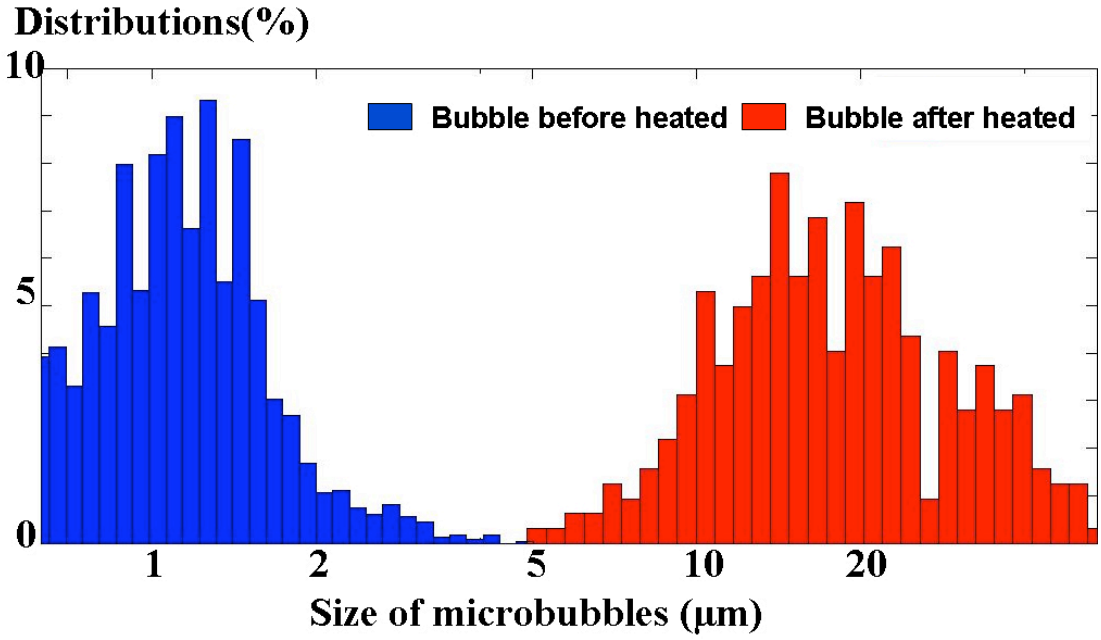

Figure 2. Size distribution of PFC encapsulated PLGA microbubbles
The mean radius of the microbubbles before being heated is 1.26 μm with a standard deviation of 0.51 μm. After being heated above 55ºC for 10 minutes, PFC inside the microbubbles evaporated and the bubbles expanded to 20.76 μm with a standard deviation of 10.44 μm.

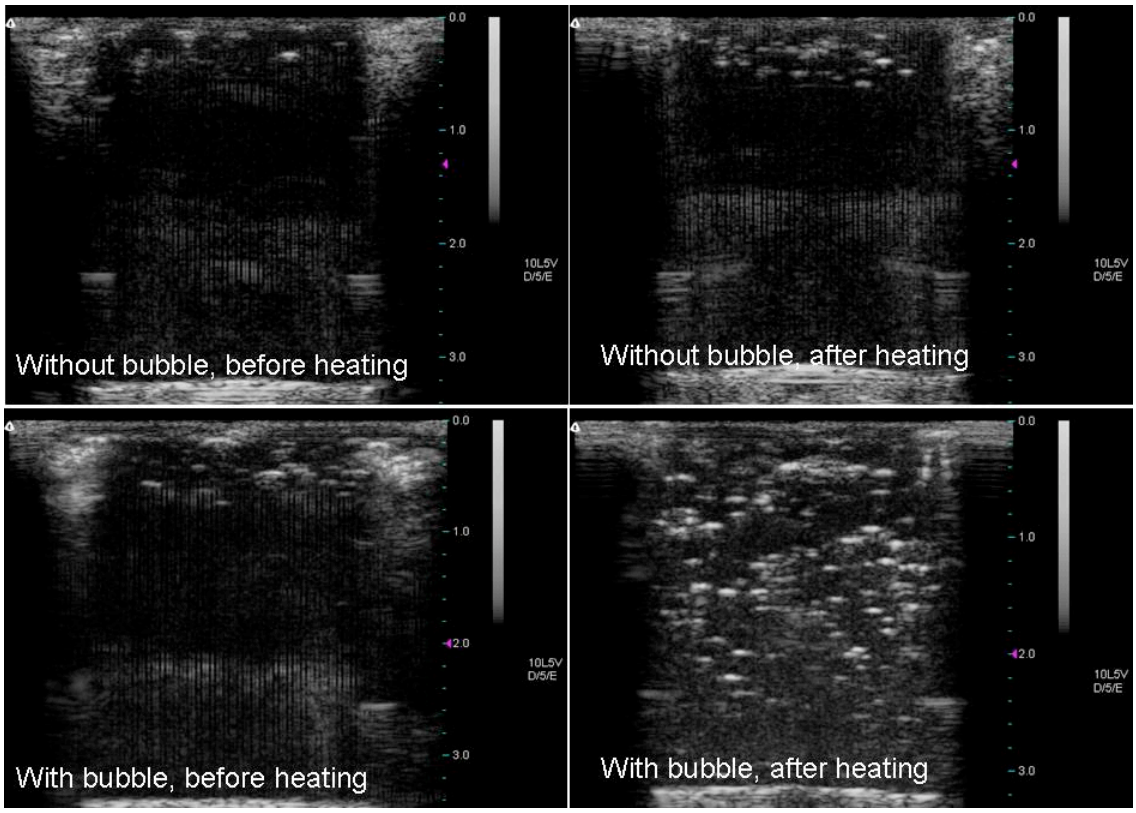

Figure3. Ultrasound image of heat-sensitive PFC encapsulated PLGA microbubbles inside agar-agar gel tissue-simulating phantom before and after being heated to 55ºC.

Fig. 3 shows the ultrasound images before and after heating for the agar-agar gel tissue-simulating phantoms with and without heat-sensitive microbubbles respectively. At the room temperature (20ºC), microbubbles in the gel phantom could not be detected by the ultrasound, indicating that the liquid PFC encapsulated microbubbles could not introduce significant ultrasound contrast. After the phantom was heated at 55ºC for 10 minutes, a number of hyperechoic areas presented in the ultrasound image, indicating the expansion of the heat-sensitive microbubbles due to PFC evaporation. In comparison, the same heating condition applied to the control phantom (i.e., the phantom without heat-sensitive microbubbles) did not introduce significant change of ultrasound contrast, ruling out the possibility of air bubble formation due to heating. The hyperechoic areas on the top of the

image are due to air bubbles existing in the ultrasound matching gel between the ultrasound probe and the phantom surface.

4. Conclusions and future works

We developed the heat-sensitive microbubbles for ablation margin assessment during a cancer ablation surgery. The heat-sensitive microbubbles, which comprise a core of liquid PFC within a biodegradable PLGA shell, were fabricated using an emulsion evaporation method. Optical microscopic imaging showed that, at the boiling point of PFC (55ºC), the microbubbles expanded from 1 μm to 20 μm due to PFC evaporation. Additionally, the microbubbles were embedded in a tissue simulating phantom made of agar-agar gel for ultrasound imaging. At room temperature, the microbubbles were not detected by the ultrasound. After being evenly heated to 55 ºC for 10 minutes, the microbubbles were clearly visualized by the ultrasound. These results demonstrate that the heat sensitive microbubbles can be potentially utilized as an ultrasound contrast agent for thermal ablation margin assessment.

Future research work includes the validation of this heat-sensitive ultrasound contrast agent for ablation margin assessment in animal models. Heat-sensitive nanobubbles with the size around 100 nm will be fabricated and conjugated with cancer-specific antibodies, such as CC49 that targets TAG-72, a human glycoprotein complex over-expressed in many epithelial-derived cancers, including colorectal, pancreatic, breast, ovarian, and gastric cancers [20]. A mathematical model will be developed to quantify the mechanism of heat-induced bubble expansion and guide the design and fabrication of heat-sensitive

nanobubbles for the designated thermal dose that matches the lethal thermal dose for effective cancer cell destruction and coagulative necrosis. Finally, the use of heat-sensitive nanobubbles for ablation margin assessment will be demonstrated using perfused tissue models and cancer xenograft mice. Clinical safety has been considered in order to facilitate the translation of this imaging technique from bench-top to bedside. Materials used for fabrication of heat-sensitive microbubbles, PFC and PLGA, are biocompatible and biodegradable materials either approved by Food and Drug Administration (FDA) or used in clinical applications. The heat-sensitive microbubbles described in this paper may revolutionize the clinical practice of minimally invasive cancer management by providing real-time intraoperative information about the tumor ablation margins.

Acknowledgements

Due to the regulation of Proceedings of Hayes Forum, Hayes Forum winners are to be the sole author on their papers. Thus here the author would like to acknowledge and thank other contributors of this paper: Dr. Ronald Xu (advisor of the author) and Dr. Jeff Xu (postdoctoral researcher) from Biomedical Engineering Department of The Ohio State University.

This research is sponsored by DOD Breast Cancer Research Program (W81XWH-07). The authors are grateful for the technical and equipment supports from Dr. Yi Zhao and Dr. Jun Liu at Biomedical Engineering Department of The Ohio State University.

References

1. Fornage, B.D., et al., *Small (= 2-cm) Breast Cancer Treated with US-guided Radiofrequency Ablation: Feasibility Study 1*. 2004, RSNA. p. 215-224.

2. Rosenberg, C., et al., *Laser Ablation of Metastatic Lesions of the Lung: Long-Term Outcome.* American Journal of Roentgenology, 2009. 192(3): p. 785-792.

3. Mougenot, C., et al., *Three-dimensional spatial and temporal temperature control with MR thermometry-guided focused ultrasound (MRgHIFU).* Magnetic Resonance in Medicine, 2008.

4. Wolf, F.J., et al., *Microwave ablation of lung malignancies: effectiveness, CT findings, and safety in 50 patients.* Radiology, 2008. 247(3): p. 871.

5. Diederich, C.J., *Thermal ablation and high-temperature thermal therapy: overview of technology and clinical implementation.* International Journal of Hyperthermia, 2005. 21(8): p. 745-754.

6. Haemmerich, D. and P.F. Laeseke, *Thermal tumour ablation: devices, clinical applications and future directions.* International Journal of Hyperthermia, 2005. 21(8): p. 755-760.

7. Brown, D.B., *Concepts, considerations, and concerns on the cutting edge of radiofrequency ablation.* Journal of Vascular and Interventional Radiology, 2005. 16(5): p. 597-613.

8. *Radiofrequency ablation for breast cancer*, in *CIGNA HEALTHCARE COVERAGE POSITION*. 2008. p. 1-8.

9. Hsu, C.P., et al., *Liver tumor gross margin identification and ablation monitoring during liver radiofrequency treatment.* Journal of Vascular and Interventional Radiology, 2005. 16(11): p. 1473-1478.

10. Wu, T., et al., *Assessment of thermal tissue ablation with MR elastography.* Magnetic Resonance in Medicine, 2001. 45(1).

11. Breen, M.S., et al., *MRI-guided thermal ablation therapy: Model and parameter estimates to predict cell death from MR thermometry images.* Annals of Biomedical Engineering, 2007. 35(8): p. 1391-1403.

12. Dewey, W.C., *Arrhenius relationships from the molecule and cell to the clinic.* International Journal of Hyperthermia, 1994. 10(4): p. 457-483.

13. de Senneville, B.D., et al., *MR thermometry for monitoring tumor ablation.* European Radiology, 2007. 17(9): p. 2401-2410.

14. Rieke, V. and K. Butts Pauly, *MR thermometry.* Journal of Magnetic Resonance Imaging, 2008. 27(2).

15. Samset, E., *Temperature mapping of thermal ablation using MRI.* Minimally invasive therapy & allied technologies: MITAT: official journal of the Society for Minimally Invasive Therapy, 2006. 15(1): p. 36.

16. Hynynen, K. and N. McDannold, *MRI guided and monitored focused ultrasound thermal ablation methods: a review of progress.* Int J Hyperthermia, 2004 20(7): p. 725-37.

17. Boss, A., et al., *Magnetic susceptibility effects on the accuracy of MR temperature monitoring by the proton resonance frequency method.* Journal of Magnetic Resonance Imaging, 2005. 22(6).

18. Poorter, J.D., *Noninvasive MRI thermometry with the proton resonance frequency method: study of susceptibility effects.* Magnetic Resonance in Medicine, 1995. 34(3).

19. Pisani, E., et al., *Polymeric nano/microcapsules of liquid perfluorocarbons for ultrasonic imaging: physical characterization.* Langmuir, 2006. 22: p. 4397-4402.

20. Zou, P., et al., *Near-Infrared Fluorescence Labeled Anti-TAG-72 Monoclonal Antibodies for Tumor Imaging in Colorectal Cancer Xenograft Mice.* Molecular pharmaceutics, 2009.